Journal of Engineering Science and Technology
Vol. 14, No. 6 (2019) 3347 - 3360

DIGITAL IMAGE WATERMARKING ALGORITHM BASED ON TEXTURE MASKING MODEL

DUJAN B. TAHA[1], TAHA BASHEER TAHA[2,*],
NAJLA BADIE AL DABAGH[3], RUZELITA NGADIRAN[4],
PHAKLEN EHKAN[4]

[1]Software Engineering Department, College of Computer Science and Mathematics, Mosul University, Iraq
[2]IT Department, Faculty of Sciences, Tishk International University, Erbil, Iraq
[3]Computer Science Department, College of Computer Science and Mathematics, Mosul University, Iraq
[4]School of Computer and Communication Engineering, University Malaysia Perlis, Perlis, Malaysia
*Corresponding Author: PhD.Taha@gmail.com

Abstract

The trade-off between invisibility and robustness in image watermarking algorithms is considered as one of the major issues in designing watermark-based copyright protection systems. Accordingly, different models had been proposed in the literature to obtain robust watermarked images while maintaining the perceptual quality. However, most of these studies are involved with complex algorithms as using multiple signal transformation tools within hybrid systems. In this paper, a low complexity texture-masking model based on Lifting Wavelet Transform (LWT) is utilized to find the blocks with the highest texture and choose them for watermark embedding. Choosing highly textured places helps to insert the watermark with a further intensity that leads to higher robustness and at the same time the Human Visual System (HVS) is less sensitive to changes in these areas. As a result, high quality watermarked images were produced in terms of objective and subjective evaluations, as the structural similarity value (SSIM) for tested images was larger than 0.99.

Keywords: Accumulated lifting differences (ALD), Copyrights protection, Image processing, Non-blind watermarking, Robust watermarking, Texture masking.

1. Introduction

With the widespread distribution of digital media in the last decades, the protection of the intellectual property rights of digital data owners became increasingly significant, and security issue is considered a rising alarm around the digital world. Digital images are considered some of the most commonly used digital data in social media and in computer applications that can easily be copied and distributed. Protecting the property rights of the owners of these images is, therefore, a subject for many researchers [1-3].

As steganography, digital image watermarking is considered as a suitable tool for copyright protection, which defined as the process of embedding piece of proprietary information within the host image in a way that it doesn't affect the perceptual quality of the image (invisible watermark) where it is embedded and in the same time it tolerates different undergoing intended or unintended distortions (robust watermark). However, the two features of invisibility and robustness are contrary, i.e., when the watermark is embedded with higher density, better robustness achieved but less invisibility. Similarly, when the watermark has low embedding intensity, better appearance can be achieved but the robustness would be limited [4, 5].

Accordingly, different algorithms had been proposed in the literature to achieve the best trade-off between invisibility and robustness, by using transform domain embedding [6, 7], hybrid embedding techniques [8, 9], or analysing perceptual factors before embedding [10, 11]. Different perceptual factors were used such as texture masking and intensity level. The human vision system (HVS) has less sensitivity if the texture is high, except the texture near edges. In addition, the human eye is less sensitive to noise in bright and dark intensities than middle intensities.

In this paper, Taha et al. [12] proposed an embedding technique, in which, using a low complexity texture masking model and referred to as accumulated lifting differences (ALD). The texture masking model is relied on integer-based lifting wavelet transform (LWT) to estimate the amount of texture in each image block. Since the human eye has less sensitivity to observe changes in highly textured areas [10], the proposed embedding algorithm calculates the highest textured blocks and embed the watermark within the approximation band coefficients of these blocks. Accordingly, embedding strength was on its higher value so more robustness could be achieved without affecting the image quality. Furthermore, in the embedding process low capacity (less number of watermark bits replicas) had been used, which results in a modification of a portion of image coefficients. The modified coefficients are within the highest texture places where the human eye has less sensitivity to alteration as mentioned earlier.

The paper was organized as follows; in the next section, literature of recent blind watermarking attempts is presented. In section three, the texture estimation model is briefly explained, while in section four the methodology of the proposed model is explained followed by experimental results and comparison in sections five and six respectively. The paper is concluded in section seven.

2. Review of Literature

Generally, image-watermarking attempts are classified into time domain and frequency domain techniques. In time-domain watermarking, the image pixels are directly modified by the value of the watermark such as significant bits modification according to the value of a binary watermark [13]. However, this method is considered vulnerable against most geometric and non-geometric attacks.

To achieve better robustness, transform domain watermarking is used, where the image is transformed into frequency coefficients using one of the transformation tools as discrete cosine transform DCT [14], discrete wavelet transforms DWT [15], or singular value decomposition SVD [16]. The watermark then is embedded into transformed frequency coefficients. The drawback of this method is the higher computation requirements in comparison to time-domain techniques.

Watermark detection can be achieved by informed (non-blind) or non-informed (blind) detectors, in informed detectors, the existing of the original image is important to extract the watermark, while in non-informed extraction, the original image is not necessary for watermark recovery [17]. In this work, informed detection was used and recent attempts were studied and analysed.

Imran et al. [18] proposed a hybrid non-blind attempt to embed the watermark into coloured images. The watermark was embedded into the singular values of discrete wavelet transform sub-band. The embedding is performed after the colour components are uncorrelated using principal component analysis. Arya et al. [19] presented another hybrid-watermarking attempt, where the DWT was utilized with DCT to achieve higher robustness and invisibility.

The watermark was embedded within an 8×8 block DCT that is applied on the approximation band of DWT. Wang et al. [20] used SVD with DWT with the aid of grey rational analysis. Watermarking bits are embedded for adjusting the largest singular values that are obtained from certain training models. Based on studies by Mekarsari et al. [21], the same hybrid of DWT and SVD was also employed, where the watermark is embedded by the SVD method within the second DWT decomposition.

Mentioned attempts used a hybrid of different signal transformation tools to achieve high robustness and invisibility. However, the combination of multiple signal transformation processes produces high complexity systems [8] that are not required in limited resources or real-time applications. Even attempts that used a single transformation such as DWT is considered a complex operation for its floating-point calculations. To solve the complexity issue, the entire design in the proposed system relies on a single and integer transformation, which is Lifting Wavelet Transform (LWT). The LWT is utilized to create the texture map and to perform the transform domain embedding at the same time, which lead to performing the process of watermarking efficiently.

3. Texture Masking

To find the highest watermark embedding intensity that cannot be perceived by human eyes, a texture masking model is utilized. The model is used to find the highest texture areas and use them for watermark embedding. The existing of more texture in a certain area means less human eye sensitivity to modifications in that area [10].

Taha et al. [12] proposed the Accumulative Lifting Differences (ALD) as a texture-masking model, which is employed in this paper for its low complexity and high good texture estimation. The model has relied on LWT, which is characterized by integer-to-integer transformation, simplicity, and it can be easily implemented in hardware as it has no floating-point and imaginary number calculations that exist in traditional Fourier-based wavelet transform.

The ALD, texture model is based on the fact that details band coefficients of LWT are used to implement the difference between linear change and actual change in image pixels intensities, i.e., higher details band coefficients indicate higher non-linearity change in image pixels. Hence, finding the variance of the non-linearity in details band coefficients in a certain region represents the amount of texture in that region.

Accordingly, the details band is portioned into 5×5 blocks, and the absolute of the difference between every two coefficients in each row is added and the calculated values are accumulated to obtain a single value for each block that represents the amount of texture. ALD equation is given as follows:

$$ALD\ (I,J)\ =\ \sum_{i=I-2}^{I+2}\sum_{j=J-1}^{J+2}|D2(i,j-1)-D2(i,j)| \quad (1)$$

where *I*, *J* are the coordinates centre coefficients of each block in details band.

4. Proposed Watermarking Model

In this section, the watermark embedding strategy is presented followed by the extraction process.

4.1. Embedding scheme

Figure 1 shows the process of embedding the watermark into the approximation band of LWT.

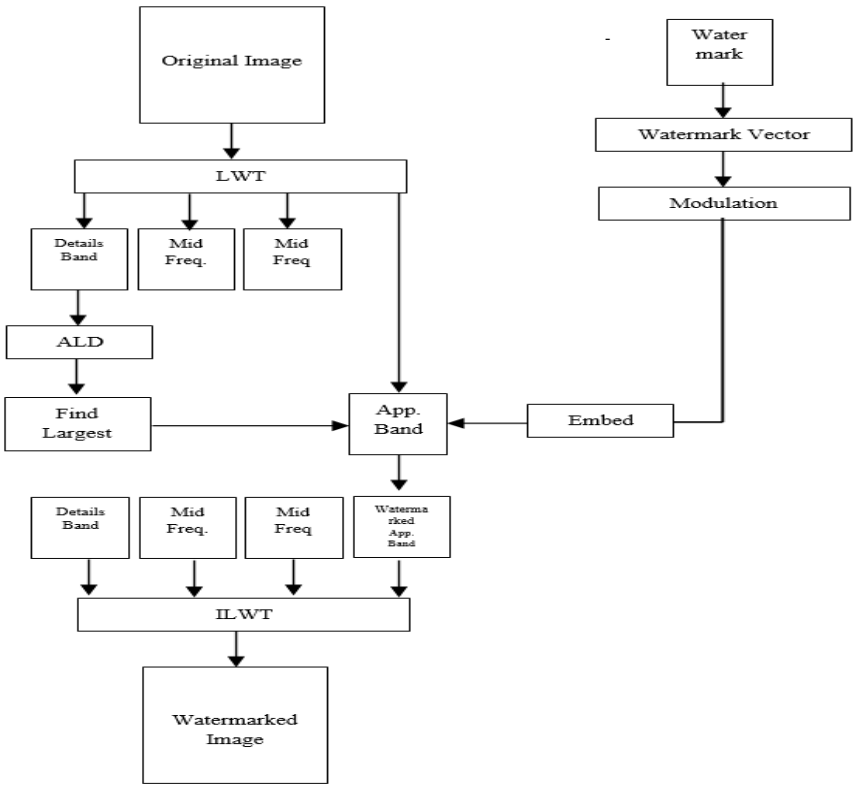

Fig. 1. Watermark embedding process.

It consists of the following steps:

- A binary watermark image is converted to a one-dimensional vector for easier embedding.
- To add an extra level of security, the vector is modulated by a pseudo-noise sequence. Modulated vector of length n is multiplied by an embedding strength constant to increase the embedding intensity.
- LWT is applied to the host image. The result is one approximation band, two middle-frequency bands, and a details band. Approximation band and Details band are used for texture masking and embedding respectively.
- Details band of LWT decomposition is used to find the texture map according to ALD equation.
- Texture blocks are sorted and the n blocks with a higher textured area are selected and marked to be used for embedding with less perceptual influence.
- In approximation band, the blocks that are equivalent to the larger n blocks of the texture masking are used for embedding. Embedding is achieved by adding/subtracting the value of the watermark vector to/from the centre.

4.2. Extraction process

The extraction process is achieved by the informed detector, where the original image is used for watermark extraction, as explained in the following:

- One LWT decomposition level is applied for each of the original and watermarked images.
- The ALD texture masking is applied to the original image to find the largest n blocks that have the most textured areas.
- The equivalent n blocks in the approximation band of each of original and watermarked images are selected and marked.
- For each block in step 3, the centre coefficient of the original image is subtracted from the centre coefficient of the watermarked image. The result is a set of positive and negative values. This difference is the effect of the adding/subtracting of the watermark bit.
- The negative value means that the watermark bit at that block is zero, otherwise, it is 1.
- The obtained vector then demodulated with the pseudo-noise signal that is the same as the one used in the embedding process.
- The watermark vector is re-arranged as a two-dimensional image.

The extraction process is shown in Fig. 2.

For RGB coloured images, images are transferred to YCbCr format. The same steps are used in embedding and extraction on the luminance component *Y*.

Luminance component values range from 0 to 255 and processed in the same way of processing values in greyscale images.

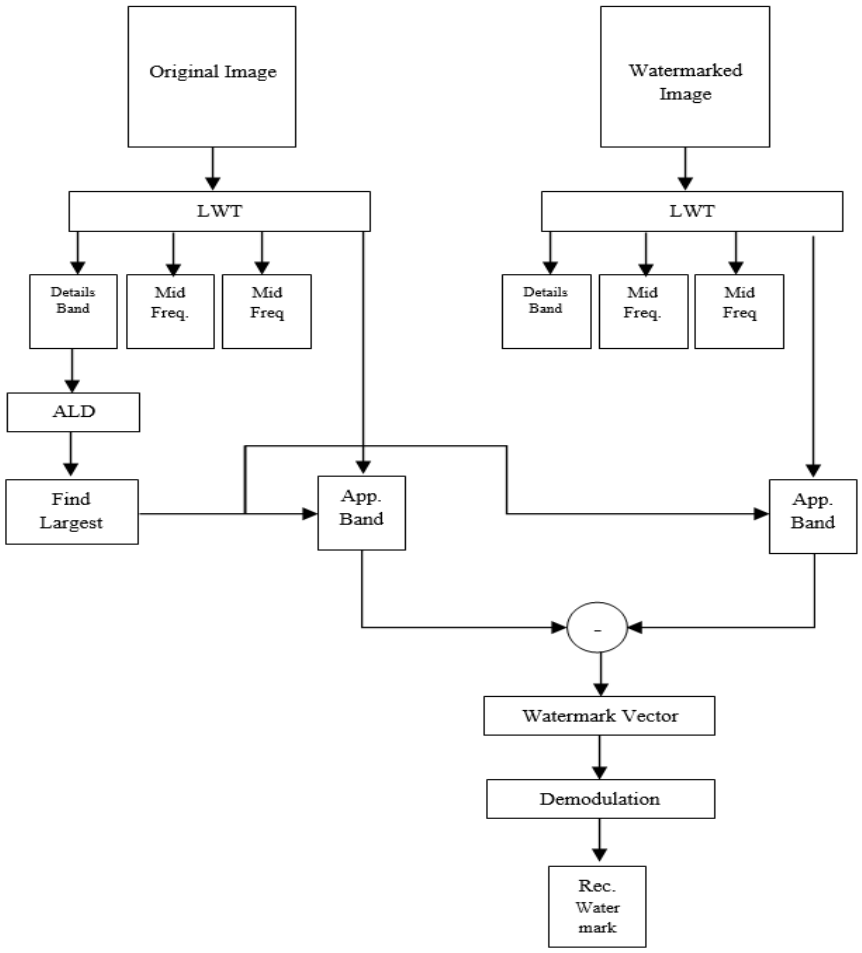

Fig. 2. Watermark extraction process.

5. Results and Discussion

In this section, the experimental results are listed, started with displaying the places where the watermark embedded according to the texture model, followed by perceptual and robustness evaluation for watermarked images.

5.1. Embedding places

The embedding process used the highest textured blocks according to Eq. (1) for watermark embedding, while the smooth areas where the human eyes have more sensitivity are excluded.

Figure 3 shows two images with textured and smooth areas where the embedding places are marked with white squares. As can be noticed, sky areas are avoided in both cases. The size of the used watermark is 32×32 (Fig. 4). Hence, 1024 blocks are used for embedding in an original image of size 512×512.

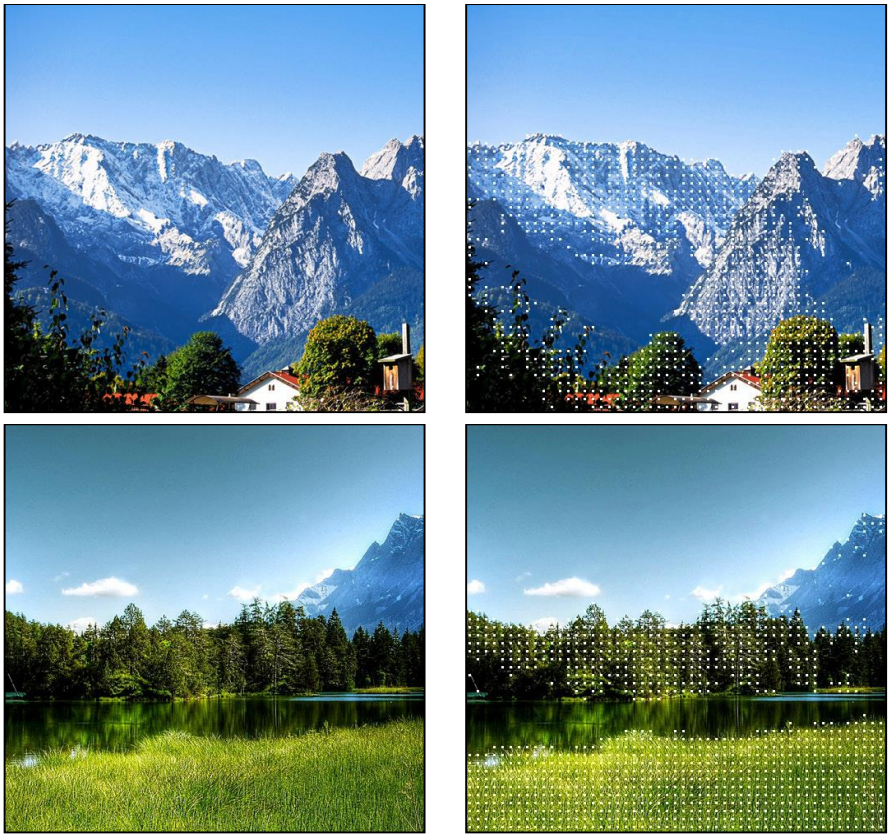

Fig. 3. Embedding places.

Fig. 4. Binary watermark.

5.2. Perceptual quality

In the embedding process, the approximation band of LWT is divided into blocks and the blocks with the largest texture are used for embedding. Furthermore, only the centre coefficient of each block is used for embedding. Accordingly, a limited portion of the image is used for watermarking and the watermark visual effect is reduced to a minimum. Tested original images are watermarked as shown in Fig. 5.

Fig. 5. Original tested images (left of column), watermarked images (right of column).

Two perceptual quality metrics are used for objective assessment, peak signal to noise ratio (PSNR) and structural similarity index (SSIM) [22].

PSNR as a quantitative measurement can be defined according to the following Eq. (2):

$$PSNR = 20\ log_{10}\left(\frac{255}{\sqrt{MSE}}\right) \tag{2}$$

Where MSE for an $m \times n$ image is given according to Eq. (3)

$$MSE = \frac{1}{m \times n}\sum_{i=1}^{m}\ \sum_{j=1}^{n} \| x(i,j) - y\ (i,j) \|^{2} \tag{3}$$

On other hand, SSIM has more realistic values in compare with PSNR [23, 24], since it takes into consideration three components, namely, luminance, contrast and

structural information, that simulate human eye observations rather than simple intensity differences used in PSNR. SSIM is given as:

$$SSIM(x,y) = \frac{(2\mu_x\mu_y+C_1)(2\sigma_{xy}+C_2)}{(\mu_x^2+\mu_y^2+C_1)(\sigma_x^2+\sigma_y^2+C_2)} \quad (4)$$

where x and y are two non-negative image signals in MSE and SSIM equations. μx, μy, are the mean intensities, σx, σy are the standard deviations for the original and distorted images respectively, $C1$, and $C2$ are constants. Table 1 lists PSNR and SSIM for different tested images.

Table 1 shows that the images have very accepted PSNR values because only limited number of pixels had been changed. The proposed watermarking algorithm changes a set of coefficients where the texture is in its maximum value, and all other images in PSNR comparison would be the same. Hence, it has high values. In terms of perceptual quality, which is measured by SSIM, all tested images have values > 0.99 as the watermark was embedded in highest textured areas where the human eye cannot perceive. This is because SSIM relies on the structure of the image, which is barely changed in the proposed method when only high texture areas were modified.

Table 1. PSNR and SSIM for tested images.

Image	PSNR(dB)	SSIM
Airplane	47.1078	0.9981
Barbara	47.1078	0.9983
Bridge	47.1168	0.9989
Downhill	47.1078	0.9975
Lax	47.1093	0.9984
Living room	47.1329	0.9978
Mandrill	47.1078	0.9992
Pirate	47.1928	0.9984
River	47.1594	0.9966
Tank	47.1089	0.9975

5.3. Robustness evaluation

To evaluate the robustness of the proposed method, different attacks had been applied on watermarked images. Tested images were exposed to following attacks, cropping by 1/16 from the left side, filtering by 3×3 gaussian filter with variance = 0.5, filtering by 3×3 low pass filter, JPEG compression with ratio of 30,50 and 70, 3×3 median filtering and salt and pepper with noise density 0.005. Recovered watermark with quality metrics is shown in Table 2. Bit Error Rate (BER) and Normalized Correlation Coefficient (NCC) were measured for the recovered watermark for different standard images after each of the mentioned attacks. BER is relied on examining the number of bit errors, as the watermark is a binary watermark, BER is considered a good measure for the similarity among the original and recovered watermarks. NCC on the other hand, is used to figure out if there is an overall correlation between two set of samples and the amount of that correlation. Equations of BER and NCC are given below:

$$BER = \frac{1}{m \times n}\sum_i^m \sum_j^n \left[W_{ij} \oplus W'_{ij}\right] \times 100\% \quad (5)$$

$$NCC = \frac{\sum_i^m \sum_j^n [W_{ij} W'_{ij}]}{\sqrt{\sum_i^m \sum_j^n (Wm_{ij})^2}\sqrt{\sum_i^m \sum_j^n (Wm'_{ij})^2}} \quad (6)$$

In both equations, *Wm*, *Wm'* are original and recovered watermarks, respectively each of size $m \times n$.

From Table 2, the watermark was 100% recovered from all the images when no attacks were applied. Low BER and high NCC values were obtained in most of other attacks, and the restored watermark image can be easily recognized. Hence, the algorithm is generally robust.

Table 2. BER and NCC for extracted watermark after applying different attacks.

Image		No Attack	Crop	Gaussian Filter	LPF	JPG30	JPG50	JPG70	Median	S&P
Airplane	BER	0	0.0225	0.0068	0.2012	0.0830	0.0186	0.0039	0.1191	0.0146
	NCC	1	0.9842	0.9952	0.8499	0.9403	0.9869	0.9973	0.9132	0.9897
										
Barbara	BER	0	0.0039	0.0850	0.3340	0.1357	0.0439	0.0020	0.2891	0.0156
	NCC	1	0.9973	0.9387	0.7411	0.9003	0.9687	0.9986	0.7794	0.9890
										
Bridge	BER	0	0.0488	0.0244	0.2871	0.1377	0.0420	0.0039	0.2588	0.0176
	NCC	1	0.9654	0.9827	0.7825	0.8995	0.9703	0.9973	0.8056	0.9876
										
Downhill	BER	0	0.0371	0.0029	0.1543	0.0635	0.0166	0.0020	0.1416	0.0137
	NCC	1	0.9737	0.9979	0.8864	0.9547	0.9883	0.9986	0.8964	0.9904
										
Lax	BER	0	0.0195	0.0322	0.2734	0.1309	0.0527	0.0059	0.2441	0.0225
	NCC	1	0.9863	0.9772	0.7940	0.9045	0.9624	0.9959	0.8161	0.9842
										
Living room	BER	0	0.0088	0.0068	0.1885	0.0781	0.0225	0.0020	0.1445	0.0186
	NCC	1	0.9938	0.9952	0.8605	0.9440	0.9842	0.9986	0.8943	0.9869
Mandrill	BER	0	0.0781	0.0645	0.3799	0.1357	0.0430	0.0020	0.3350	0.0205
	NCC	1	0.9440	0.9539	0.7023	0.9006	0.9695	0.9986	0.7409	0.9855
Pirate	BER	0	0.0186	0.0088	0.1963	0.0986	0.0313	0.0039	0.1533	0.0117
	NCC	1	0.9870	0.9938	0.8551	0.9287	0.9778	0.9973	0.8877	0.9918
River	BER	0	0.0811	0.0059	0.1309	0.0996	0.0186	0.0059	0.1172	0.0176
	NCC	1	0.9419	0.9959	0.9044	0.9282	0.9869	0.9959	0.9149	0.9876
Tank	BER	0	0.0059	0	0.1270	0.0801	0.0254	0.0049	0.1309	0.0186
	NCC	1	0.9959	1	0.9078	0.9424	0.9821	0.9966	0.9047	0.9869

The average of BER and NCC for all attacks have been depicted in Figs. 6 and 7 respectively, which shows higher BER and lower NCC after applying low pass filtering and median filtering. For low pass filtering, lower robustness occurred since the function of the filter is to remove the high-frequency components, where a large portion of highly textured areas exist.

Hence, these blocks have been affected. For median filtering, the filter is used to modify the centre value according to the mean of the window of the filter, and since the embedding is depending on a single insertion but in high intensity. Using median filtering will change this value to the mean and reduce the embedding power.

The watermark was extracted with better quality in other attacks and the best could be seen in salt and pepper attack since only a small portion of the image is used for embedding and the extracted watermark will not be affected unless the noise was on the place where the watermark bit is embedded. In general, the watermark was robust against most attacks and it still exists unless the watermarked image had been distorted.

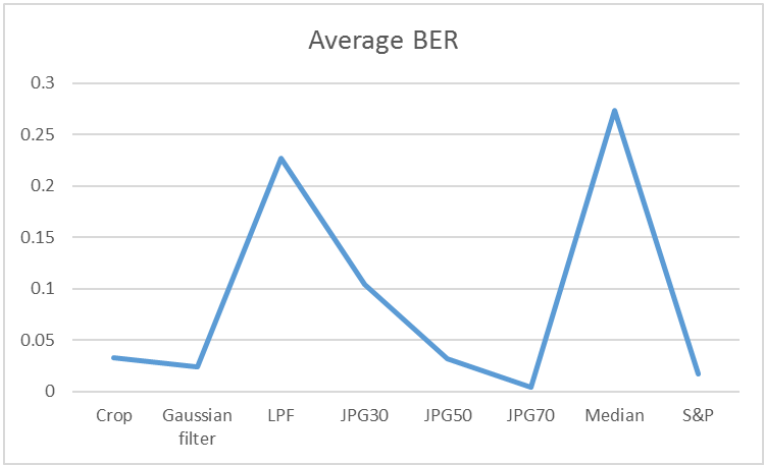

Fig. 6. Average BER for recovered watermark.

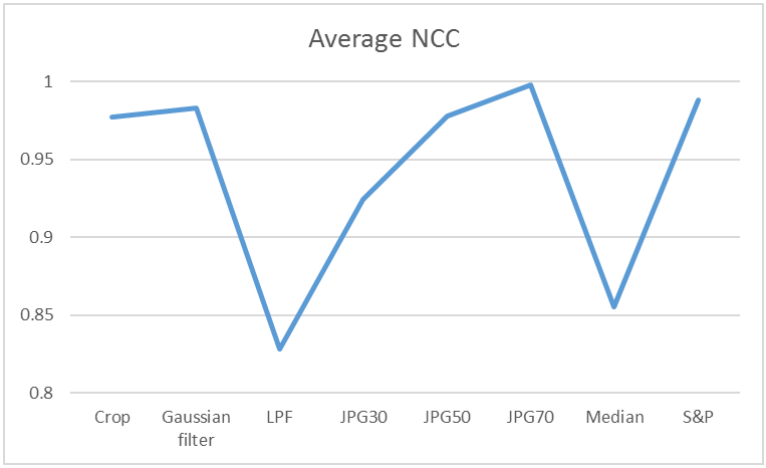

Fig. 7. Average NCC for recovered watermark.

6. Model Comparison

The proposed watermarking model was compared with the recent non-blind study presented by Wang et al. [20] in terms of watermarked image quality, robustness and simplicity. The objective quality comparison of the watermarked images between the two models is initiated using PSNR of eight standard images (Pirate, Mandrill, Downhill, living room, airplane, Barbara, Lax and Lena) as shown in Fig. 8. The proposed model has higher PSNR values in all tested images. The reason for this priority is that the proposed model uses a limited portion of the image for watermark embedding. Hence, a higher signal to noise ratio was obtained. In term of robustness, although there are no full references to all attacks on all tested images in the model presented by Wang et al. [20], listed results show that the compared model has higher NCC values for the recovered watermark after applying some attacks as JPEG compression and median filter. In cropping attack, the results depend on the places of cropping since the proposed method has different places of embedding according to texture mask existing. In terms of design complexity, the proposed model has a priority since only the integer, simplified type of DWT has been used, while according to Wang et al. [20], a hybrid of SVD and DWT were utilized. As a future work, algorithm's security can be enhanced using encryption and/or watermark distribution by applying different transformation as Arnold transform [25].

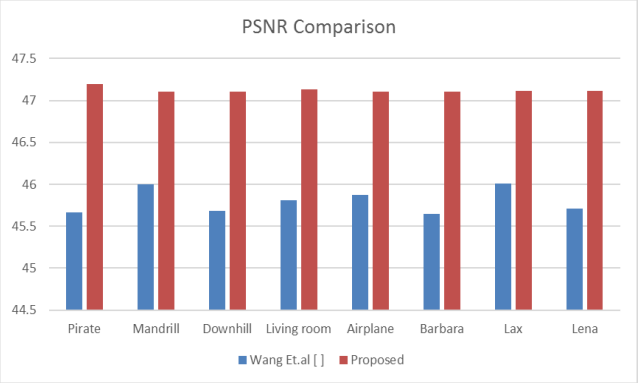

Fig. 8. PSNR comparison with Wang et al. [20].

7. Conclusion

In this paper, an image watermarking scheme based on texture estimation model is presented. The host image blocks are sorted according to the texture amount by the aid of ALD texture masking model. Then the watermark was embedded within the blocks with the highest texture as the human visual system has less sensitivity to noise in highly textured areas. In contrary to recently presented methods that are relied on complex or hybrid methods, all the processes of the proposed system were based on integer calculations, and the LWT was utilized twice in creating the texture mask and in the embedding process. The experimental results show that the proposed method produced watermarked images with high robustness against different attacks and at the same time has high perceptual quality in terms of objective and subjective evaluations. As future work, the proposed system can be enhanced by employing edge detection techniques to exclude edges from texture areas as the HVS is more sensitive to change near edges. In addition, using blind extracting method will free more memory while implementing the system. The security of the algorithm can be enhanced using encryption or watermark random distribution.

References

1. Cox, I.J.; Miller, M.L.; Bloom, J.A.; Fridrich, J.; and Kalker, T. (2007). *Digital watermarking and steganography*. San Francisco, California, United States of America: Morgan Kaufmann Publishers, Inc.
2. Sahu, A.K.; and Swain, G. (2019). A novel n-rightmost bit replacement image steganography technique. *3D Research*, 10(1), Article 211.
3. Mukherjee, S.; Roy, S.; and Sanyal, G. (2018). Image steganography using mid position value technique. *Procedia Computer Science*, 132, 461-468.
4. Sahu, A.K.; and Swain, G. (2016). A review on LSB substitution and PVD based image steganography techniques. *Indonesian Journal of Electrical Engineering and Computer Science*, 2(3), 712-719.
5. Woo, C.-S. (2007). Digital image watermarking methods for copyright protection and authentication. *Doctoral Dissertation. Faculty of Information Technology, Queensland University of Technology*, Brisbane, Queensland, Australia.
6. Kishore, P.V.V.; Srivathsav, P.D.; Manikanta, M.; Venkatram, N.; Reddy, L.S.S.; Goutham; E.N.D., Devi, D.K.; and Sastry, A.S.C.S. (2015). Medical image watermarking with psnr optimization in wavelet domain based on bat algorithm. *Journal of Theoretical and Applied Information Technology*, 80(3), 528-543.
7. Moosazadeh, M.; and Ekbatanifard, G. (2017). An improved robust image watermarking method using DCT and YCoCg-R color space. *Optik*, 140, 975-988.
8. Roy, S.; and Pal, A.K. (2017). A robust blind hybrid image watermarking scheme in RDWT-DCT domain using Arnold scrambling. *Multimedia Tools and Applications*, 76(3), 3577-3616.
9. Poonam; Arora, S.M. (2018). A DWT-SVD based robust digital watermarking for digital images. *Procedia Computer Science*, 132, 1441-1448.
10. Barni, M.; Bartolini, F.; and Piva, A. (2001). Improved wavelet-based watermarking through pixel-wise masking. *IEEE Transactions on Image Processing*, 10(5), 783-791.
11. Akhbari, B.; and Ghaemmaghami, S. (2005). Watermarking of still images in wavelet domain based on entropy masking model. *Proceedings of the TENCON 2005-2005 IEEE Region Conference*. 10, Melbourne, Queensland, Australia,. 1-6.
12. Taha, T.; Ehkan, P.; and Ngadiran, R. (2017). A new perceptual mapping model using lifting wavelet transform. *MATEC Web of Conferences*, 140, 01036.
13. Tirkel, A.Z.; Rankin, G.A.; van Schyndel, R.M.; Ho, W.J.; Mee, N.R.A.; and Osborne, C.F. (1993). Electronic watermark. *Proceedings of the Conference on Digital Image Computing, Technology and Applications (DICTA)*. Sydney, Australia, 666-673.
14. Parah, S.A.; Sheikh, J.A.; Loan, N.A., and Bhat, G.M. (2016). Robust and blind watermarking technique in DCT domain using inter-block coefficient differencing. *Digital Signal Processing*, 53, 11-24.
15. Moon, H.S.; Sohn, M.H.; and Jang, D.S. (2004). DWT-based image watermarking for copyright protection. *Proceedings of the International Conference on AI, Simulation, and Planning in High Autonomy Systems*. Jeju Island, Korea, 490-497.
16. Shirvanian, M.; and Azar, F.T. (2008). Adaptive SVD-based digital image watermarking. *Proceedings of the International Workshop on Digital Watermarking (IWDW)*. Busan, Korea, 113-123.

17. Minamoto, T.; and Ohura, R. (2012). A non-blind digital image watermarking method based on the dual-tree complex discrete wavelet transform and interval arithmetic. *Proceedings of the Ninth International Conference on Information Technology-New Generations (ITNG).* Las Vegas, Nevada, United States of America, 623-628.
18. Imran, M.; Ghafoor, A.; and Khokher, M.R. (2012). A robust non-blind color image watermarking scheme. *Proceedings of the 12th International Conference on Control Automation Robotics and Vision (ICARCV).* Guangzhou, China, 1392-1396.
19. Arya, R.K.; Singh, S., and Saharan; R. (2015). A secure non-blind block based digital image watermarking technique using DWT and DCT (ICACCI). *Proceedings of the International Conference on Advances in Computing, Communications and Informatics (ICACCI).* Kerala, India, 2042-2048.
20. Wang, Q.; Ma, J.; Wang, X.; and Zhao, F. (2017). Image watermarking algorithm based on grey relational analysis and singular value decomposition in wavelet domain. *Proceedings of the International Conference on Grey Systems and Intelligent Services (GSIS).* Stockholm, Sweden, 94-98.
21. Mekarsari, Y.A.; Setiadi, D.R.I.M.; Sari, C.A.; Rachmawanto, E.H.; and Muljono. (2018). Non-blind RGB image watermarking technique using 2-level discrete wavelet transform and singular value decomposition. *Proceedings of the International Conference on Information and Communications Technology* (ICOIACT). Jogkajarta, Indonesia, 623-627.
22. Wang, Z.; Bovik, A.C.; Sheikh, H.R.; and Simoncelli, E.P. (2004). Image quality assessment: From error visibility to structural similarity. *IEEE Transactions on Image Processing*, 13(4), 600-612.
23. Kotevski, Z.; and Mitrevski, P. (2010). Experimental comparison of PSNR and SSIM metrics for video quality estimation. *ICT Innovations*, 357-366.
24. Silpa, K.; and Mastani, S.A. (2012). Comparison of image quality metrics. *International Journal of Engineering Research and Technology (IJERT)*, 1(4), 5 pages.
25. Pandey, M.K.; Parmar, G.; and Gupta, R. (2018). A robust non-blind hybrid color image watermarking with arnold transform. *ICTACT Journal on Image and Video Processing*, 9(1), 1814-1820.